Impact of head modeling and sensor types in localizing human gamma-band oscillations*

Mideksa, K.G., Hoogenboom, N., Hellriegel, H., Krause, H.,
Schnitzler, A., Deuschl, G., Raethjen, J., Heute, U., and Muthuraman, M.

Abstract— **An effective mechanism in neuronal communication is oscillatory neuronal synchronization. The neuronal gamma-band (30-100 Hz) synchronization is associated with attention which is induced by a certain visual stimuli. Numerous studies have shown that the gamma-band activity is observed in the visual cortex. However, impact of different head modeling techniques and sensor types to localize gamma-band activity have not yet been reported. To do this, the brain activity was recorded using 306 magnetoencephalography (MEG) sensors, consisting of 102 magnetometers and 102 pairs of planar gradiometers (one measuring the derivative of the magnetic field along the latitude and the other along the longitude), and the data were analyzed with respect to time, frequency, and location of the strongest response. The spherical head models with a single-shell and overlapping spheres (local sphere) have been used as a forward model for calculating the external magnetic fields generated from the gamma-band activity. For each sensor type, the subject-specific frequency range of the gamma-band activity was obtained from the spectral analysis. The identified frequency range of interest with the highest gamma-band activity is then localized using a spatial-filtering technique known as dynamic imaging of coherent sources (DICS). The source analysis for all the subjects revealed that the gradiometer sensors which measure the derivative along the longitude, showed sources close to the visual cortex (cuneus) as compared to the other gradiometer sensors which measure the derivative along the latitude. However, using the magnetometer sensors, it was not possible to localize the sources in the region of interest. When comparing the two head models, the local-sphere model helps in localizing the source more focally as compared to the single-shell head model.**

I. INTRODUCTION

Gamma-band (30-100 Hz) synchronization is a fundamental process of activated cortical neuronal networks. A series of studies demonstrated that the gamma frequency oscillations affect neuronal interactions and thereby are involved in several central cognitive functions, including visual perception [1], attention [2-4], as well as motor control [5-6]. Neuronal synchronization in the gamma-frequency range has been originally observed in the visual cortex of anesthetized cats and monkeys [7]. Recently, the study of gamma-band activity with electroencephalography (EEG) and magnetoencephalography (MEG) in humans has gained interest and has been localized in the visual cortex similar to that of the animals [8-11].

The non-invasive detection of these gamma-frequency oscillations needs a highly optimized paradigm that can induce strong gamma-band activity as there are also some physiological artifacts occurring at the same frequency band [12-13]. Thus, in this study we used a task design that has been proven to induce strong visual cortical gamma-band activity [9] and used cuneus, a region of visual cortex that is mainly responsible in the perception of motion, as the region of interest.

In order to localize neuronal current activity, a valid head model (forward model), which calculates the electromagnetic potentials or fields generated from a current source, is necessary irrespective of the inverse technique used.

This paper investigates the impact of using different head modeling techniques (single-shell and local sphere) and different sensor types from a multichannel MEG measurement system, consisting of magnetometers and pairs of planar gradiometers, in localizing the gamma-band activity through the application of a beamformer technique known as DICS.

II. DATA ACQUISITION

MEG signals were recorded using the Elekta Neuromag whole-head system. The system contains three sensor types at one location measuring independent information as shown in Fig. 1. The first sensor type consists of 102 magnetometers (MEG1) which measure the magnetic flux perpendicular to its surface and the other sensor pairs consist of 204 planar gradiometers which measure the spatial gradient (102 gradiometers measuring the gradient along the latitude (MEG2) and 102 gradiometers measuring the gradient along the longitude (MEG3)). The data were sampled at 1000 Hz.

The experiment was performed by five healthy subjects (four females and one male). Their age ranged from 25 to 36 years (31$\pm$5.15). Each trial started with the presentation of a fixation point. After a baseline period of 1000 ms, the fixation point was replaced by a foveal circular sine wave grating (diameter: 5; spatial frequency: 2 cycles/deg; contrast: 100%) and made to accelerate contracting towards the fixation point (velocity step to 2.2 deg/s) for 50 to

*Research supported by SFB 855 Project D2.

Mideksa, K.G. and Heute, U. are with the Institute for Digital Signal Processing and System Theory, Faculty of Engineering, Christian-Albrechts-University of Kiel, 24105 Kiel, Germany. kgm at tf.uni-kiel.de, uh at tf.uni-kiel.de

Hellriegel, H., Deuschl, G., Raethjen, J., and Muthuraman, M. are with the Department of Neurology, Christian-Albrechts-university of Kiel, 24105 Kiel, Germany. h.hellriegel at neurologie.uni-kiel.de, g.deuschl at neurologie.uni-kiel.de, j.raethjen at neurologie.uni-kiel.de, m.muthuraman at neurologie.uni-kiel.de

Hoogenboom, N., Krause, H., and Schnitzler, A. are with the Department of Neurology, Heinrich-Heine University Düsseldorf, 40225 Düsseldorf, Germany. Nienke.Hoogenboom at med.uni-duesseldorf.de, Holger.Krause at med.uni-duesseldorf.de, schnitza at uni-duesseldorf.de

978-1-4244-7929-0/14/$26.00 ©2014 IEEE

1500 ms. The subjects were asked to fixate for the entire experiment and press a button with their right index finger within 500 ms of this acceleration. The stimulus was turned off after a response was given and was followed by a resting period of 1000 ms in which subjects were given visual feedback about the correctness of their response and were asked to blink. Each subject completed 80-150 trials. The recording session lasted for about 50 min.

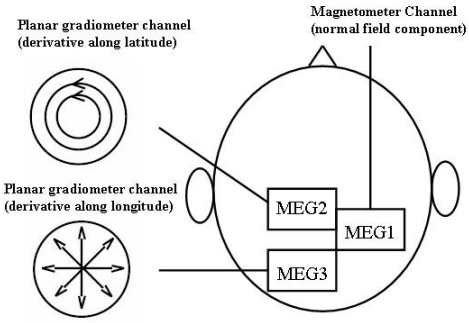

Fig. 1. Sensor nomenclature of the MEG system. MEG1 representing the magnetometer sensors measuring the normal field component, MEG2 and MEG3 representing the gradiometer sensors measuring the spatial gradient along the latitude and longitude respectively.

III. METHODS

Three main analysis steps were carried out in order to localize the gamma-band activity in all the subjects: time-course power analysis at the sensor level, head modeling, and source analysis underlying the spectral component obtained from the sensor-level analysis. All the analyses were performed using the FieldTrip open-source Matlab toolbox (http://fieldtrip.fcdonders.nl/).

A. Time-Frequency Analysis

To detect the latency and frequency range of the gamma-band activity which are not known a priori, we performed a time-frequency representation (TFR) of the signal. The method is based on multitapering of the signal, which allows a better control of time and frequency smoothing, to reveal the time-varying estimate of the power of the signal at a given frequency. Calculating the TFRs power is done using a sliding time window, where each windowed trial is multiplied with a taper in the frequency domain and finally averaged over all the tapered spectra. In this study, we used a 50 ms sliding window and a Hanning taper. The TFRs power were represented as a percent change with respect to the baseline (1000 ms before stimulus onset, considering 0 ms as the onset onset for the stimulus). We used the data from 1000 ms before stimulus onset until 1500 ms after stimulus onset. Power estimates were averaged across 32 parieto-occipital sensors for each sensor type separately (MEG163**X**, MEG164**X**, MEG171**X**, MEG172**X**, MEG173**X**, MEG174**X**, MEG183**X**, MEG184**X**, MEG191**X**, MEG192**X**, MEG193**X**, MEG194**X**, MEG201**X**, MEG202**X**, MEG203**X**, MEG204**X**, MEG211**X**, MEG212**X**, MEG213**X**, MEG214**X**, MEG223**X**, MEG224**X**, MEG231**X**, MEG232**X**, MEG233**X**, MEG234**X**, MEG243**X**, MEG244**X**, MEG251**X**, MEG252**X**, MEG253**X**, MEG254**X**). The least-significant digit in the naming of the individual sensors is used to distinguish the three orthogonal sensors. '**X**' = 1 is used for magnetometer sensors (MEG1) and '**X**' = 2 and '**X**' = 3 are used for the planar gradiometers (MEG2 and MEG3 respectively).

B. Head Modeling

There are various methods to construct a head model (forward model) which maps current sources within the brain to the electromagnetic potentials or fields. Based on the geometry assumed, they can be solved either analytically or numerically [14]. Analytical solutions exist for simplified geometries, e.g., when the head is assumed to be a sphere. Because of their simplicity and ease of computation, spherical head models (single-shell) have traditionally been used for approximating the human head in EEG and MEG analyses, as compared to the numerical techniques (boundary element method (BEM) and finite element method (FEM)). Since MEG shows a weak dependence on the electrical properties of the brain compartments, a single-shell head model is normally adequate in obtaining a good approximation of the forward solution.

The magnetic field $\mathbf{B}$ is calculated from the total current density $\mathbf{J}$ using the Biot-Savart law:

$$\mathbf{B} = \frac{\mu_0}{4\pi} \int \frac{\mathbf{J} \times \mathbf{R}}{d^3} dV, \tag{1}$$

where μ_0 is the free-space magnetic permeability, $\mathbf{R}$ is the vector from the source point to the field point, and d is the distance between them. $\mathbf{J} = \mathbf{J_i} - \sigma \nabla V$, $\mathbf{J_i}$ is the induced current density and $-\sigma \nabla V$ is the Ohmic current with conductivity σ. The potential V is obtained by solving the Poisson's equation:

$$\nabla \cdot \sigma \nabla V = \nabla \cdot \mathbf{J_i}. \tag{2}$$

Another simple head model is the overlapping or local sphere model, in which a single sphere is fitted on a sensor-by-sensor basis using a set of grid points within the brain instead of using a single best-fitting sphere for all sensors as in the case of the single-shell model [15].

In this study, the brain region was extracted first from each of the subjects' structural magnetic resonance images (MRI), and the forward model is then solved analytically using both the single-shell and the local-sphere head models separately.

C. Source Localization

In order to locate the gamma-band activity, we used a beamformer technique known as dynamic imaging of coherent sources (DICS). It is quite often used in localizing the coherent network of sources for a specific frequency band by imaging power and coherence estimates within the brain [16-17]. In this study, we used only the power information to observe the location of the source that is responsible for the gamma activity upon visual stimulation for the identified frequency range. DICS is based on adaptive spatial filters to map the underlying neural activity to the electromagnetic

field on the surface. These spatial filters optimally pass signals from the desired frequency band while attenuating signals from other frequency bands.

The entire volume of all the subject's brain was divided into a three-dimensional grid of 1 mm and the source strength was estimated at each grid point taking into account the solution from the forward model and the cross-spectral density between all the MEG signals over the frequency range of interest, obtained from the time-frequency analysis. The cross-spectral densities for all the sensor combinations was computed from the Fourier-transformed signals of each trial, separately for each sensor type. The spatial distribution of the power of the neuronal sources, which is represented as a contrast with respect to the baseline, was then overlaid on a structural image of the subject's brain.

IV. RESULTS

A. Time-frequency Analysis

The time-frequency analysis for all the sensor types confirms that the stimulus-related response is in the gamma frequency range. The time course of gamma-band activity due to the visual stimuli, for one of the representative subjects, is illustrated in the time-frequency plot shown in Fig. 2. It can be seen that the gamma-band activity is maintained throughout the post-stimulus duration. The gamma power over the parieto-occipital sensors (visual cortical areas), expressed in percent change with respect to the baseline, was different for all the subjects, mainly concentrating between 40 to 80 Hz. We also observed a clear gamma activity in all the subjects taking the average of all 32 parieto-occipital gradiometer sensors (MEG2 and MEG3 separately) as compared to the magnetometer sensors (MEG1), where we were not able to see a clear gamma activity from the average of all 32 parieto-occipital magnetometer sensors. Only the average of 1 to 5 sensors were used to observe a clear gamma activity for the MEG1 sensors. In one of the subjects, we were not able to see a gamma-band activity from any of the parieto-occipital magnetometer sensors.

B. Source Localization

To estimate the location of the source of the gamma-band activity, we applied DICS on the three sensor types (MEG1, MEG2, and MEG3) for the single-shell and local sphere head models separately. Fig. 3 shows the results obtained, for one of the representative subjects, for the estimated source power at 72±6 Hz. Comparing the three sensor types, MEG2 and MEG3 sensors were able to localize the gamma-band activity as expected in the deeper slice of the brain at the visual cortex (cuneus) as compared to the MEG1 sensor types which localize it on the top-most slice of the brain (parietal region) for both head models. We also observed that the MEG3 sensor types showed sources close to the cuneus as compared to the MEG2 sensor types for all the subjects. This result was supported by calculating the euclidean distance between the reference MNI coordinate (x,y,z), midline of the cuneus separating the two hemispheres (obtained from the standard template: 2,-86,26 mm) to that of the MNI coordinate of the strongest response (voxel with the highest power occurring either in the right or left hemisphere of the visual cortex) obtained from the source analysis for each subject separately (mean±std: MEG1=50.61±23.11, MEG2=44.75±10.99, MEG3=35.13±3.34). All the sensor types showed no significant difference in the power of the strongest response relative to the baseline using both head-modeling techniques. Comparing the two head models, using the local-sphere head model helps in localizing the source more focally as compared to using the single-shell head model. This result was supported, for all the subjects, by estimating the number of voxels activated over the whole brain for each case as illustrated in table 1. The criterion used to estimate the number of highly activated voxels was by taking those voxels which showed 50% of the highest relative power change with respect to the baseline. The smaller the number of voxels, the more focal we see the source in the expected region of interest, which is the cuneus. For the subject which did not show the gamma-band activity in the spectral analysis of the MEG1 sensor types, we were also not able to localize the source.

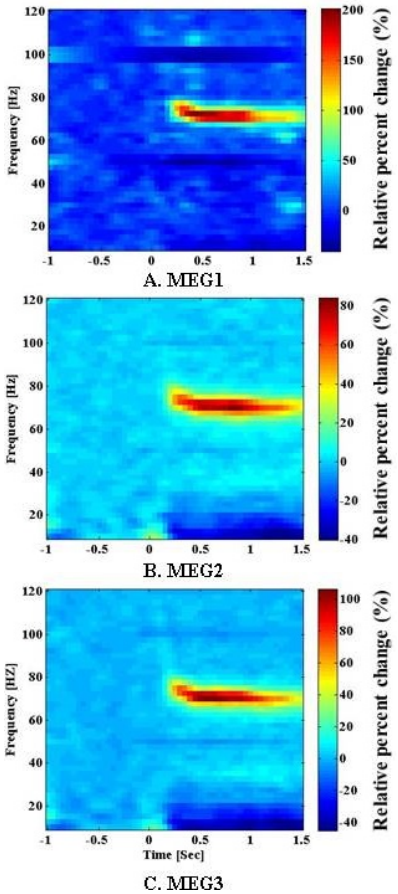

Fig. 2. Time-frequency plot representing the gamma power across the average of selected parieto-occipital sensors for one of the representative subjects. Baseline: -1 to 0 sec, Stimulus: 0 to 1.5 sec. The colorbars represent the percent change with respect to the baseline. A. Magnetometer sensors (average of 5 parieto-occipital MEG1 sensor types), B. Gradiometer sensors (average of 32 parieto-occipital MEG2 sensor types), C. Gradiometer sensors (average of 32 parieto-occipital MEG3 sensor types).

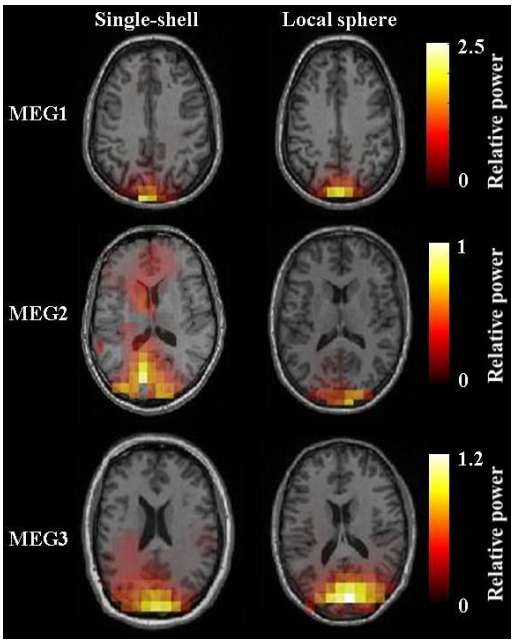

Fig. 3. Estimated sources of visually induced gamma-band activity on a single slice plot of a single-shell head model in the first column and local sphere in the second column for one of the representative subject. The first, second, and third row show sources as measured using MEG1, MEG2, and MEG3 sensor types respectively. The colorbars indicate the relative power change with respect to the baseline.

TABLE I

NUMBER OF VOXELS ACTIVATED DURING THE SOURCE LOCALIZATION FOR THE THREE SENSOR TYPES (MEG1, MEG2, AND MEG3) USING THE SINGLE-SHELL AND LOCAL SPHERE HEAD MODELS

Subjects	MEG1		MEG2		MEG3	
	Single	Local	Single	Local	Single	Local
1	1060	856	1010	942	1060	952
2	900	772	727	698	902	832
3	-	-	745	651	738	613
4	256	191	374	330	340	333
5	1372	1196	1267	996	1142	1036

V. CONCLUSIONS

We have analyzed the impact of different head modeling techniques (single-shell and local sphere head models) and different sensor types (magnetometeres (MEG1) and pairs of gradiometers (MEG2 and MEG3)) in localizing the gamma-oscillatory activity using multichannel MEG recordings. We applied the adaptive spatial-filtering technique known as DICS to estimate the sources of the gamma-band activity. From our time-frequency analysis results, we observed clear gamma-band activity, from the average of all 32 parieto-occipital sensors, for both the gradiometer sensors separately (MEG2 and MEG3 sensor types), in all the subjects, as compared to magnetometer sensors (MEG1 sensor types). Both MEG2 and MEG3 sensor types were able to localize the source in the expected visual cortical area, where MEG3 localize it close to the region of interest, that is, the cuneus. In contrast, MEG1 sensor types localize sources in the parietal region. For this kind of oscillatory activity, it implies that the dipolar sources are oriented more in the longitudinal direction which can be easily picked up by the MEG3 sensor types. We also observed that using a local-sphere head model helps in localizing the source more focally in the region of interest as compared to using a single-shell head model.

ACKNOWLEDGMENT

Support from the German Research Council (Deutsche Forschungsgemeinschaft, DFG, SFB 855, Project D2) is gratefully acknowledged.

REFERENCES

[1] L. Melloni, C. Molina, M. Pena, D. Torres, W. Singer, E. Rodriguez, Synchronization of neural activity across cortical areas correlates with conscious perception, J. Neurosci., vol. 27, pp. 2858-2865, Mar. 2007.

[2] O. Jensen, J. Kaiser, J.P. Lachaux, Human gamma-frequency oscillations associated with attention and memory, Trends Neurosci., vol. 30, no. 7, pp. 317-324, Jul. 2007.

[3] P. Fries, J.H. Reynolds, A.E. Rorie, R. Desimone, Modulation of oscillatory neuronal synchronization by selective visual attention, Science, vol. 291, no. 5508, pp. 1560-1563, Feb. 2001.

[4] B. Pesaran, J.S. Pezaris, M. Sahani, P.P. Mitra, R.A. Andersen, Temporal structure in neuronal activity during working memory in macaque parietal cortex, Nat. Neurosci., vol. 5, no. 8, pp. 805-811, Aug. 2002.

[5] S.D. Muthukumaraswamy, K.D. Singh, J.B. Swettenham, D.K. Jones, Visual gamma oscillations and evoked responses: variability, repeatability and structural MRI correlates, Neuroimage, vol. 49, no. 4, pp. 3349-3357, Feb. 2010.

[6] D. Cheyne, S. Bells, P. Ferrari, W. Gaetz, A.C. Bostan, Self-paced movements induce high-frequency gamma oscillations in primary motor cortex, Neuroimage, vol. 42, no. 1, pp. 332-342, Aug. 2008.

[7] C.M. Gray, P. Knig, A.K. Engel, W. Singer, Oscillatory responses in cat visual cortex exhibit inter-columnar synchronization which reflects global stimulus properties, Nature, vol. 338, no. 6213, pp. 334-337, Mar. 1989.

[8] P. Adjamian, I.E. Holliday, G.R. Barnes, A. Hillebrand, A. Hadjipapas, K.D. Singh, Induced visual illusions and gamma oscillations in human primary visual cortex, Eur. J. Neurosci., vol. 20, no. 2, pp. 587-592, Jul. 2004.

[9] N. Hoogenboom, J.M. Schoffelen, R. Oostenveld, L.M. Parkes, P. Fries, Localizing human visual gamma-band activity in frequency, time and space, Neuroimage, vol. 29, no. 3, pp. 764-773, Feb. 2006.

[10] A. Hadjipapas, P. Adjamian, J.B. Swettenham, I.E. Holliday, G.R. Barnes, Stimuli of varying spatial scale induce gamma activity with distinct temporal characteristics in human visual cortex, Neuroimage, vol. 35, no. 2, pp. 518-530, Apr. 2007.

[11] P. Fries, R. Scheeringa, R. Oostenveld, Finding gamma, Neuron, vol. 58, no. 3, pp. 303-305, May 2008.

[12] S. Yuval-Greenberg, O. Tomer, A.S. Keren, I. Nelken, L.Y. Deouell, Transient induced gamma-band response in EEG as a manifestation of miniature saccades, Neuron, vol. 58, no. 3, pp. 429-441, May 2008.

[13] E.M. Whitham, et al., Scalp electrical recording during paralysis: quantitative evidence that EEG frequencies above 20 Hz are contaminated by EMG, Clin. Neurophysiol., vol. 118, no. 8, pp. 1877-1888, Aug. 2007.

[14] F. Meneghini, F. Vatta, F. Esposito, S. Mininel and F. D. Salle, Comparison between realistic and spherical approaches in EEG forward modeling, Biomed. Tech. (Berl), vol. 55, no. 3, pp. 133-146, Jun. 2010.

[15] M.X. Huang, J.C. Mosher, R. Leahy, A sensor-weighted overlapping-sphere head model and exhaustive head model comparison for MEG, Phys. Med. Biol., vol. 44, no. 2, pp. 423-440, Feb. 1999.

[16] J. Gross, J. Kujala, M. Hämäläinen, L. Timmermann, A. Schnitzler, R. Salmelin, Dynamic imaging of coherent sources: Studying neural interactions in the human brain, Proc. Natl. Acad. Sci. U.S.A., vol. 98, no. 2, pp. 694-699, Jan. 2001.

[17] J. Gross, L. Timmermann, J. Kujala, M. Dirks, F. Schmitz, R. Salmelin, A. Schnitzler, The neural basis of intermittent motor control in humans, Proc. Natl. Acad. Sci. U.S.A., vol. 99, no. 4, pp. 2299-2302, Feb. 2002.